6th European Conference on Computational Mechanics (ECCM 6)
7th European Conference on Computational Fluid Dynamics (ECFD 7)
11 – 15 June 2018, Glasgow, UK

FEATURES OF THE SETTLEMENT SCHEME ASPIRATION OF ELEVATOR OVERLOADS

OLGA A. AVERKOVA[1], IVAN N. LOGACHEV[1], KONSTANTIN I. LOGACHEV[1], VALERYI A. UVAROV[1] AND ARSLAN M. ZIGANSHIN[2]

[1] Belgorod State Technological University named after V.G. Shukhov,
(BSTU named after V.G. Shukhov) 308012 Belgorod, Russia
e-mail: kilogachev@mail.ru, web page: http://www.bstu.ru

[2] Kazan State University of Architecture and Engineering, Russia,
Zelenaya Str., 1 - 420043 Kazan, Tatarstan, Russia. E-mail: amziganshin@kgasu.ru

Key words: Aspiration, bulk material transfer, air suction.
Abstract. The schemes of aspiration of elevator overloads have been developing. Balance equations of ventilation of aspiration covers are compiled. The system of equations for determination of the volumes of ventilating air for a standard node overload are formulated and solved. Ways of reducing productivity of aspiration systems are offered and analytically substantiated.

1 INTRODUCTION

This article is a logical follow-up of our research works [1-2], considering the air ejection phenomenon (air entrainment with loose material flow) in bucket elevators. The purpose of this work is developing a design model for analytical and numerical justification of ways to reduce the aspiration systems performance [3-4] at transloading loose materials in bucket elevators.

2 AERODYNAMIC PERFORMANCE OF ELEVATOR BUCKETS

Obtaining data on the coefficient c_{b} is a prerequisite for determining the parameters M_1 and M_2 describing the behavior of air cross-flow patterns in elevator enclosures. This coefficient represents the ratio of frontal drag force to the dynamic pressure of air multiplied by mid-section area of a bucket traveling at a relative velocity w:

$$c_{\text{b}} = \frac{R}{F_{\text{b}} \dfrac{w^2 \rho}{2}}, \qquad w = v_e - u\,. \tag{1}$$

In case of fixed buckets, airflow with the same velocity w within elevator enclosure with a cross-sectional size of S produces drag forces equal in their absolute value to the force R:

$$R = \Delta p_{\text{b}} \cdot S\,, \tag{2}$$

where $\Delta p_{\text{к}}$ are pressure losses caused by the drag of the fixed end. In the design practice these

are determined using the local resistance coefficient

$$\Delta p_{\text{b}} = \zeta_{\text{b}} \frac{w^2 \rho}{2}. \tag{3}$$

Substitution of (2) and (3) into (1) results in the ratio:

$$c_{\text{b}} = \frac{S}{F_{\text{b}}} \zeta_{\text{b}}, \tag{4}$$

which can be used to determine c_{b} given known LRC of an enclosure member with a fixed bucket. We'll use experimental data on orifice drag [5] determining LRC as a function of orifice area and cross-sectional size of the duct S. In our case the orifice area would be:

$$S_{\text{o}} = S - A_{\text{b}} \cdot B_{\text{b}} = S - F_{\text{b}}. \tag{5}$$

Bucket dimensions in lengthwise cross-section will be compared either with a rectangle (Fig. 1 *a*), a sharp-edged trapezoid (Fig. 1 *b*) if the surrounding airflow around passes along the head side of the bucket, or a dull-edged shape if the surrounding airflow passes along the back side of the bucket (Fig. 1. *c*). In the first case we'll use the results for an orifice with beaded edges in a direct pipe [5]:

$$\zeta_{\text{b}} = \left(\zeta_{\text{o}} + \lambda \frac{l}{D_{\text{h}}} \right) \left(\frac{S}{S_0} \right)^2, \tag{6}$$

where

$$\zeta_{\text{o}} = 0.5 \left(1 - \frac{S}{S_{\text{o}}} \right) + \left(1 - \frac{S_{\text{o}}}{S} \right)^2 + \tau \sqrt{1 - \frac{S_{\text{o}}}{S}} \left(1 - \frac{S_{\text{o}}}{S} \right); \tag{7}$$

D_{h} is hydraulic diameter of the orifice, equal in our case to:

$$D_{\text{h}} = \frac{4 S_{\text{o}}}{\Pi_{\text{o}}} = \frac{2 S_{\text{o}}}{a + b + A_{\text{b}}}; \tag{8}$$

λ is the coefficient of air friction against bucket walls ($\lambda \approx 0{,}02$);

τ is a correction coefficient that depends on bucket depth (Table 1).

Table 1

l/D_{h}	0	0.2	0.4	0.6	0.8	1.0	1.4	2	≥ 3
τ	1.35	1.22	1.10	0.84	0.42	0.24	0.1	0.02	0

It is possible to use a simpler model of pressure losses inside an orifice with sharp edges [5]

$$\zeta_{\text{b}} = \bar{\zeta}_{\text{b}} = \left(1 + 0.707 \sqrt{1 - \frac{S_{\text{o}}}{S}} - \frac{S_{\text{o}}}{S} \right)^2 \left(\frac{S}{S_{\text{o}}} \right)^2. \tag{9}$$

Let $A_{\text{k}} = 250$ mm; $B_{\text{b}} = 500$ mm; $l = 300$ mm; $a = 400$ mm; $b = 700$ mm, then

$F_b = 0.125$ m^2; $S = 0.28$ m^2; $S_0 = 0.28 - 0.125 = 0.155$ m^2; $D_h = \frac{2 \cdot 0.155}{0.4 + 0.7 + 0.25} = 0.23$ m; $\frac{l}{D_h} = 0.3/0.23 = 1.3$; $\tau \approx 0.08$.

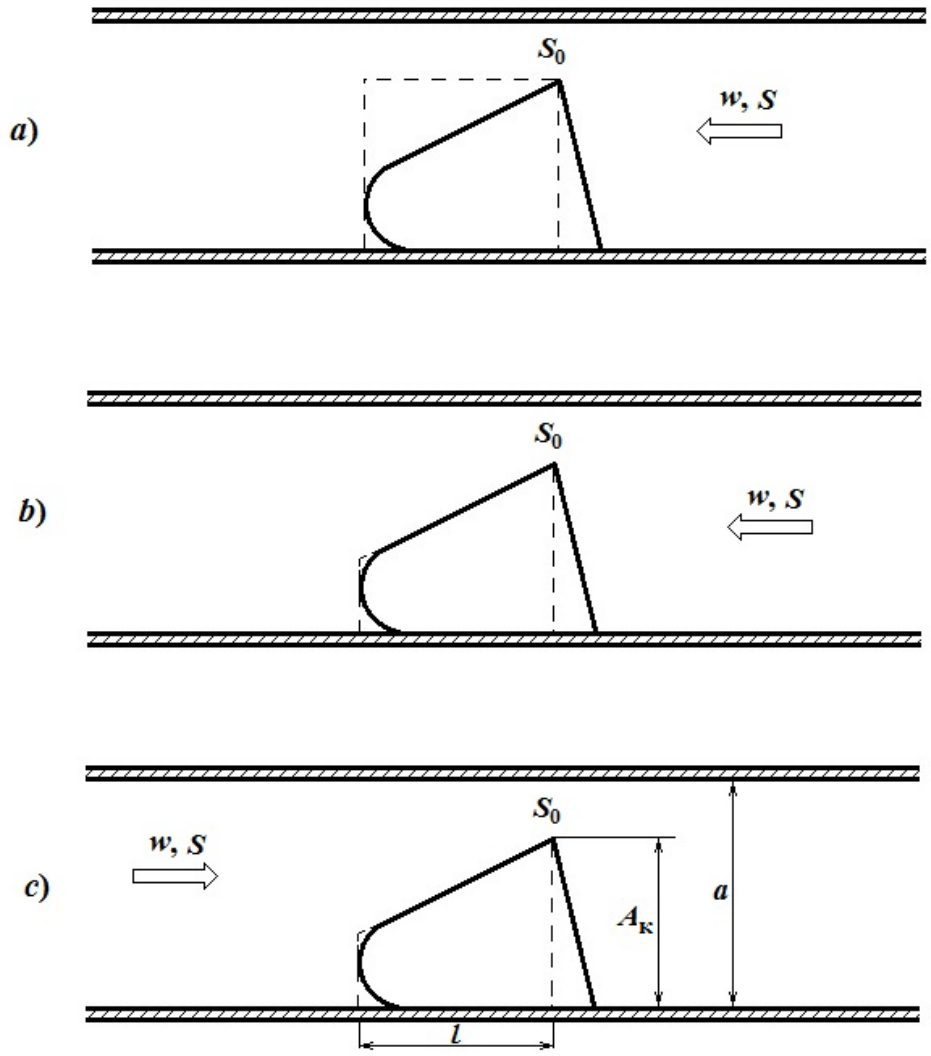

Figure 1: Chart of airflow surrounding a fixed bucket inside an enclosure

If these values were substituted into formulas (7), (6) and (9), they would resolve into: $\zeta_o = 0.947$; $\zeta_b = 1.56$; $\bar{\zeta}_b = 2.75$, i.e. formula (9) would produce somewhat higher LRC values.

For a flow surrounding the back side of a bucket we'll use experimental data for an orifice with edges chamfered downstream [5]:

$$\zeta_{\text{b}} = \vec{\zeta}_{\text{b}} = \left(1+\sqrt{\xi\left(1-\frac{S_{\text{o}}}{S}\right)}-\frac{S_{\text{o}}}{S}\right)^2\left(\frac{S_{\text{o}}}{S}\right)^2, \tag{10}$$

where $\xi = f\left(l/D_{\text{h}}\right)$ is the adjustment coefficient (Table 2).

Table 2

l/D_{b}	0.01	0.02	0.03	0.04	0.06	0.08	0.12	0.16
ξ	0.46	0.42	0.38	0.35	0.29	0.23	0.16	0.13

The following ratio will result if formulas (9) and (10) are compared:

$$\frac{\overleftarrow{\zeta}_{\text{b}}}{\vec{\zeta}} = \left(\frac{1+0.707\sqrt{\left(1-\frac{S_{\text{o}}}{S}\right)}-\frac{S_{\text{o}}}{S}}{1+\sqrt{\xi}\sqrt{1-\frac{S_{\text{o}}}{S}}-\frac{S_{\text{o}}}{S}}\right)^2. \tag{11}$$

As charts (Fig.2) illustrate, the aerodynamic drag of a bucket increases noticeably when airflow impinges on the receiving orifice. The deeper the bucket, the more noticeable is the difference. It is unfortunate that formula (10) is only applicable at $l/D_{\text{h}} \le 1.6$ whereas l/D_{h} is much greater in grain elevators ($l/D_{\text{h}} > 0.5$).

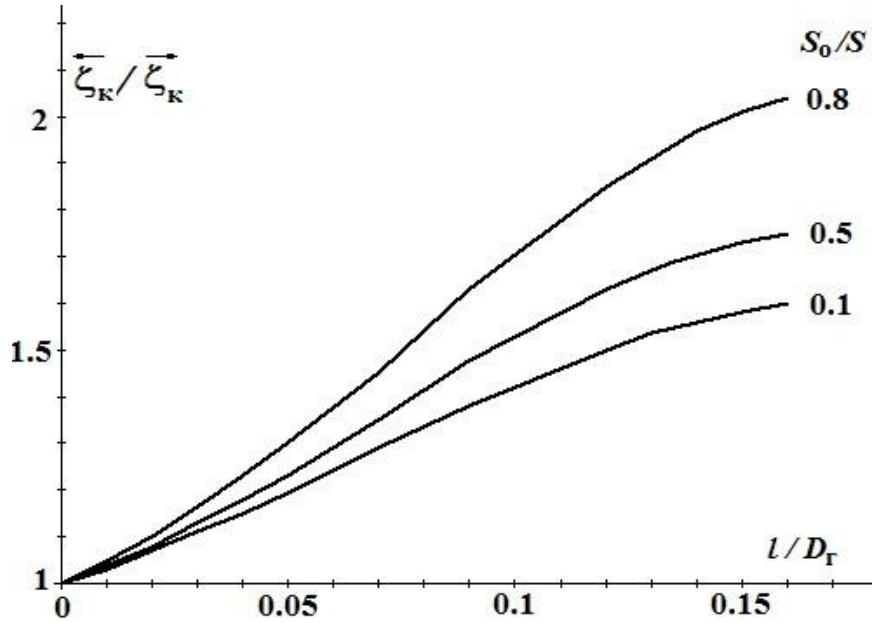

Figure 2: Variation in LRC of elevator bucket as a function of airflow and depth (according to the data provided by Prof., Dr. I.E. Idelchik)

Let's now compare the results in the particular case of thin partitions with the resistance of

a gate (damper) in a straight pipe [5]. For a rectangular duct ($a/b = 0.5$), the LRC of a single-side gate depends on the relative gap height h/a. Listed in Table 3 (assuming identical $h/a \equiv S_o/S$) are LRCs of gate (ζ_g), LRCs of a sharp-edged orifice $\overleftarrow{\zeta}_b$) computed using formula (9), LRCs of an orifice with beaded edges (ζ_b) computed using formula (6) at $l/D_h = 0$ ($\tau = 1.35$), LRCs of an orifice chamfered downstream ($\vec{\zeta}_b$) computed using formula (10) at $l/D_h = 0.01$ ($\xi = 0.46$).

Table 3

h/a	0.1	0.15	0.20	0.30	0.40	0.50	0.60	0.70	0.80	0.90
ζ_g	105	51.5	30.6	13.5	6.85	3.34	1.73	0.83	0.32	0.09
$\overleftarrow{\zeta}_b$	246.7	100	51.3	18.5	8.23	4.0	2.0	0.96	0.42	0.13
ζ_b	241.3	98	50	18.1	8.04	3.91	1.95	0.94	0.41	0.13
$\vec{\zeta}_b$	238.2	96.7	49.5	17.8	7.92	3.84	1.91	0.92	0.40	0.12

It can be seen from this data that LRCs of thin orifices are for all practical purposes in an adequate agreement within a wide range of relative orifice areas (within $0.1 \le S_o/S \le 0.9$). However the LRC of an orifice significantly exceeds that LRC of a gate, especially within the range of small orifices (at $S_o/S < 0.2$), despite the two being quite similar structurally.

To examine the effect that elongation of a body has on its frontal drag coefficient and resistance to airflow, it would be instructive to consider the aerodynamic resistance of classic bodies: the hemisphere and the cylinder. At $\mathrm{Re} = \dfrac{wd_p}{v} = 4 \cdot 10^5$, boundless airflow around a convex hemisphere of a cup (so that the cup opens leeward) would encounter a drag coefficient of $\vec{c}_p = 0.36$ [5]. With the same Reynolds number but with oppositely directed airflow (the cup opens windward), this coefficient quadruples ($\overleftarrow{c}_p = 1.44$).

For an airflow around a smooth circular cylinder in parallel to its generatrix (i.e. perpendicular to the impermeable cylinder base), the drag coefficient first declines with increasing cylinder length but then increases. A cylinder with a length equal to double its base diameter would have a minimal drag coefficient $c_p = 0.85$ (for a thin disk-like cylinder, $c_d = 1$, same in the case of cylinder length equal to seven times its diameter).

So, despite the apparent structural similarity of partitions surveyed, LRC values differ sharply in the case of beaded (lengthy) partitions. Therefore, great care is needed when using these findings to quantitatively estimate the drag of various bucket designs as they may be filled up with grain to a different extent. It would be much more reliable to investigate individual cases experimentally.

3 FEATURES OF THE PROPOSED DESIGN FOR ASPIRATION LAYOUT OF GRAIN ELEVATORS

Dust releases during handling of unheated grain are usually contained by sucking air from bottom cowls (Fig. 3):

- from the cowl of elevator loading location (from the elevator "boot" enclosure)
- from the cowl of conveyor loading location (from the cowl of the boot of elevator discharge chute).

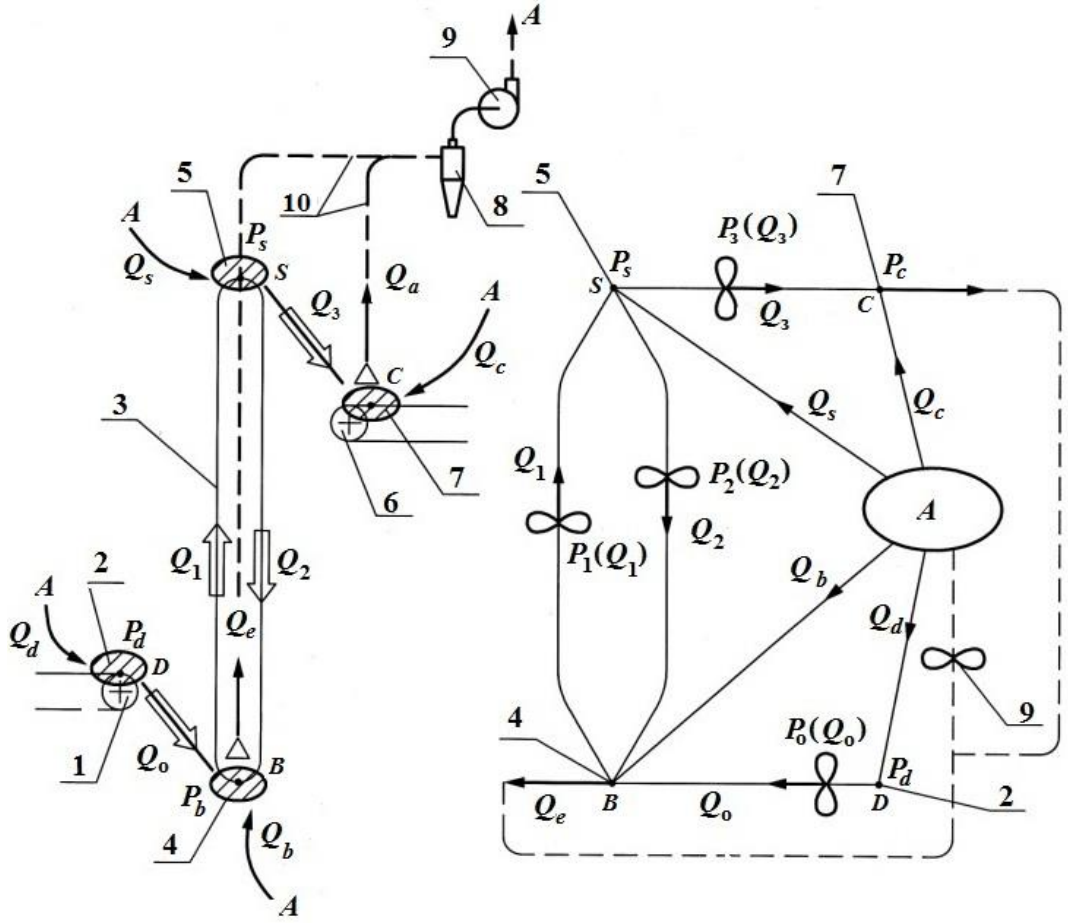

a) *b*)

Figure 3: Aspiration design (*a*) and its aerodynamic equivalent (*b*): 1 – belt-conveyor feeder; 2 – cowl of the driving drum of belt-conveyor feeder; 3 – (bucket) elevator; 4 – cowl of elevator boot; 5 – upper cowl of bucket elevator (cowl of the drive sprocket of elevator); 6 – belt conveyor; 7 – cowl of the filling location; 8 – dust trap (cyclone); 9 – aspiration system fan; 10 – air ducts

Let's assume that, in the case of unaspirated cowls, a sufficient negative pressure (preventing escape of dust-laden air through poorly sealed locations in cowls) is maintained inside the cowl of the bottom conveyor driving drum (feeding mechanism) and inside the enclosure of the elevator driving drum (the "head" of the elevator) by cross-flows of air through adjacent chutes and elevator enclosures.

The air cross-flow pattern through these ducts is determined by the following combined equations for the dynamics of air in ducts:

$$P_{\mathrm{s}} - P_{\mathrm{b}} - P_2\left(Q_2\right) = R_2 Q_2^2; \tag{12}$$

$$P_{\mathrm{b}} - P_{\mathrm{s}} + P_1\left(Q_1\right) = R_1 Q_1^2; \tag{13}$$

$$P_{\mathrm{s}} - P_{\mathrm{c}} + P_3\left(Q_3\right) = R_3 Q_3^2; \tag{14}$$

$$P_{\mathrm{d}} - P_{\mathrm{b}} + P_{\mathrm{o}}\left(Q_{\mathrm{o}}\right) = R_{\mathrm{o}} Q_{\mathrm{o}}^2; \tag{15}$$

$$P_A - P_{\mathrm{c}} = R_{\mathrm{c}} Q_{\mathrm{c}}^2; \tag{16}$$

$$P_A - P_{\mathrm{s}} = R_{\mathrm{s}} Q_{\mathrm{s}}^2; \tag{17}$$

$$P_A - P_{\mathrm{b}} = R_{\mathrm{b}} Q_{\mathrm{b}}^2; \tag{18}$$

$$P_A - P_{\mathrm{d}} = R_{\mathrm{d}} Q_{\mathrm{d}}^2 \tag{19}$$

and balance of air in junction points

$$Q_e + Q_1 - Q_2 - Q_{\mathrm{o}} - Q_{\mathrm{b}} = 0; \tag{20}$$

$$Q_3 + Q_2 - Q_1 - Q_{\mathrm{s}} = 0; \tag{21}$$

$$Q_a - Q_3 - Q_{\mathrm{c}} = 0; \tag{22}$$

$$Q_0 - Q_{\mathrm{d}} = 0; \tag{23}$$

$$Q_{\mathrm{s}} + Q_{\mathrm{c}} + Q_{\mathrm{d}} + Q_{\mathrm{b}} - Q_a - Q_e = 0, \tag{24}$$

where $P_{\mathrm{s}}, P_{\mathrm{b}}, P_{\mathrm{d}}, P_{\mathrm{c}}$ are the respective absolute pressures within the cowls of elevator head and boot, upper and lower conveyor feeder driving drums (Pa).

Q_0, Q_1, Q_2, Q_3 are the respective flow rates of air arriving through the loading chute, enclosures of carrying and return runs of elevator conveyor, and the discharge chute (m^3/s)

$Q_{\mathrm{d}}, Q_{\mathrm{b}}, Q_{\mathrm{s}}, Q_{\mathrm{c}}$ are flow rates of air coming in through leaky areas in cowls of the feeder drive drum, elevator boot and head, and upper conveyor loading location (m^3/s)

Q_e, Q_a are the respective flow rates of air evacuated by the suction system from the elevator boot cowl and the location of grain dumping onto upper conveyor (m^3/s)

R_0, R_1, R_2, R_3 are the respective aerodynamic properties of the loading chute, enclosures of the carrying and return runs of elevator conveyor, and the discharge chute ($Pa/(m^3/s)^2$) that determine resistance posed by ducts to cross-flows of air

$$R_0 = \zeta_0 \frac{\rho}{2S_0^2}; \tag{25}$$

$$R_1 = \sum \zeta_1 \frac{\rho}{2S_1^2}; \tag{26}$$

$$R_2 = \sum \zeta_2 \frac{\rho}{2S_2^2}; \tag{27}$$

$$R_3 = \zeta_3 \frac{\rho}{2S_3^2}; \tag{28}$$

$\zeta_0, \sum\zeta_1, \sum\zeta_2, \zeta_3$ are the respective sum totals of LRCs for the loading chute, enclosures of carrying and return runs of elevator conveyor, and discharge chute;

S_0, S_1, S_2, S_3 are the respective cross-sectional areas of the loading chute, enclosures of carrying and return runs of elevator conveyor, and discharge chute (m^2);

ρ is air density (kg/m^3);

P_A is atmospheric pressure (absolute pressure in the room) (Pa);

R_d, R_b, R_s, R_c are the respective aerodynamic properties of leaky areas in the feeder drive drum cowl, elevator boot and head cowls, and upper conveyor loading location cowl ($Pa/(m^3/s)^2$), which determine the resistance to ingress of air into cowls through leaky areas:

$$R_d = \zeta_d \frac{\rho}{2F_d^2}; \tag{29}$$

$$R_b = \zeta_b \frac{\rho}{2F_b^2}; \tag{30}$$

$$R_s = \zeta_s \frac{\rho}{2F_s^2}; \tag{31}$$

$$R_c = \zeta_c \frac{\rho}{2F_c^2}; \tag{32}$$

$\zeta_d, \zeta_b, \zeta_s, \zeta_c$ are LRCs of leakage areas in the respective cowls, accepted equal to the LRC of a hole in a thin wall [5]

$$\zeta_d = \zeta_b = \zeta_s = \zeta_c = 2.4; \tag{33}$$

F_d, F_b, F_s, F_c are the respective leakage areas of the feeder cowl, elevator boot and head cowls, and upper conveyor cowl (m^2);

$P_0(Q_0), P_1(Q_1), P_2(Q_2), P_3(Q_3)$ are ejection pressures as functions of airflows in the loading chute, inside enclosures of the carrying and return runs of elevator conveyor, and in the discharge chute, respectively (Pa).

While combined equations (12)-(15) describe the cross-flow of air through ducts, the second set of equations that includes equalities (16)-(19) determines flow rates of air entering through leakage areas of the respective cowls due to differential pressure. Combined, relations (20)-(24) comprise balance equations of the respective air flow rates: in boot (20) and head (21) cowls of the elevator, in the conveyor cowl (22), in the feeder cowl (23) and, finally, inside an imagined junction point (24) for air flows in the atmosphere.

The latter equation can be transformed into the relation:

$$Q_e + Q_a = Q_d + Q_s + Q_c, \tag{34}$$

describing an obvious but nevertheless a rather important fact: the total performance of an aspiration unit is determined by the sum total of flow rates of air entering the cowl system

through leaky areas. In addition, in order to reduce power consumption of the aspiration system and to bring down dust releases, it is necessary to seal not only cowls provided with local suction units for evacuating air but also to adequately seal aspirated cowls.

For the purpose of arriving at computational relations for determining flow rates of air in ducts, we'll put forth, based on (21) and (23), that:

$$Q_{\text{s}} = Q_3 + Q_2 - Q_1 = Q_3 + \Delta Q; \quad \Delta Q = Q_2 - Q_1; \tag{35}$$

$$Q_{\text{d}} = Q_0 . \tag{36}$$

Keeping in mind that differential pressures in left-hand sides of equations (16)-(19) represent negative pressures in the respective cowls, we'll rewrite the second set of combined equations as follows:

$$h_{\text{d}} = R_{\text{d}} Q_{\text{d}}^2 = R_{\text{d}} Q_0^2; \tag{37}$$

$$h_{\text{b}} = R_{\text{b}} Q_{\text{b}}^2; \tag{38}$$

$$h_{\text{s}} = R_{\text{s}} Q_{\text{s}}^2 = R_{\text{s}} \left(Q_3 + \Delta Q\right)^2; \tag{39}$$

$$h_{\text{c}} = R_{\text{c}} Q_{\text{c}}^2, \tag{40}$$

where $h_{\text{п}}, h_{\text{в}}$ are negative pressures established within unaspirated cowls of elevator feeder due to cross-flows of air through adjacent ducts (Pa); $h_{\text{н}}, h_{\text{к}}$ are negative pressures maintained in aspirated cowls of elevator boot and upper conveyor loading location by a running fan (Pa).

The first set of combined equations (12)…(15) will be rewritten in view of these relations as follows:

$$h_{\text{b}} + P_0\left(Q_0\right) = \left(R_{\text{d}} + R_0\right) Q_0^2; \tag{41}$$

$$P_1\left(Q_1\right) + P_{\text{s}} Q_{\text{s}}^2 - h_{\text{b}} = R_1 Q_1^2; \tag{42}$$

$$P_2\left(Q_2\right) - R_{\text{s}} Q_{\text{s}}^2 + h_{\text{b}} = R_2 Q_2^2; \tag{43}$$

$$P_3\left(Q_3\right) + h_{\text{c}} - R_{\text{s}} Q_{\text{s}}^2 = R_3 Q_3^2. \tag{44}$$

By assuming h_{b} and h_{c} to be predefined and solving these combined equations in view of equation (35), we'll determine the sought flow rates of air in ducts Q_0, Q_1, Q_2 and Q_3.

In order to combined equations for computation purposes, we'll explicitly present the formulas for determining ejection pressures in ducts:

$$P_1\left(Q_1\right) = E_1\left(L_1 - Q_1\right)^2; \tag{45}$$

$$P_2\left(Q_2\right) = E_2\left(L_2 - Q_2\right)^2, \tag{46}$$

with the following notational simplification:

$$L_1 = v_e S_1, \tag{47}$$

$$L_2 = v_e S_2, \tag{48}$$

$$E_1 = M_1 \frac{\rho}{2S_1^2}, \tag{49}$$

$$E_2 = M_2 \frac{\rho}{2S_2^2}. \tag{50}$$

For loading and discharge chutes:

$$P_0(Q_0) = E_0 \left[|L_{k0} - Q_0|^3 - |L_{n0} - Q_0|^3 \right]; \tag{51}$$

$$P_3(Q_3) = E_3 \left[|L_{k3} - Q_3|^3 - |L_{n3} - Q_3|^3 \right]; \tag{52}$$

$$L_{ki} = v_{ki} S_i; \quad L_{ni} = v_{ni} S_i; \tag{53}$$

$$E_i = K_0 \psi_{yi} \beta_{ki} \frac{v_{ki} \rho}{4 d_e a_{\tau i} S_i^3}; \tag{54}$$

$$\beta_{ki} = \frac{G_m}{\rho_m S_i v_{ki}}. \tag{55}$$

Here a subscript $i = 0$ is used to refer to the parameters of a loose-matter flow in the loading chute, and $i = 3$ refers to the flow in the discharge chute.

After simple algebraic transformations in view of relations (45), (46), (51), (52), combined equations (41)-(44) can be presented as the following computational set:

$$E_0 \left[|L_{k0} - Q_0|^3 - |L_{n0} - Q_0|^3 \right] + h_b = (R_d + R_0) Q_0^2; \tag{56}$$

$$E_1 (L_1 - Q_1)^2 + E_2 (L_2 - Q_2)^2 = R_1 Q_1^2 + R_2 Q_2^2; \tag{57}$$

$$E_2 (L_2 - Q_2)^2 + h_b - R_s (Q_3 + Q_2 - Q_1)^2 = R_2 Q_2^2; \tag{58}$$

$$E_3 \left[|L_{k3} - Q_3|^3 - |L_{n3} - Q_3|^3 \right] + E_1 (L_1 - Q_1)^2 + h_c - h_b = R_1 Q_1^2 + R_3 Q_3^2. \tag{59}$$

However the first equation of this set is independent of others and can be formal solved as follows: $Q_0 = \sqrt{\dfrac{E_0 \left[|L_{k0} - Q_0|^3 - |L_{n0} - Q_0|^3 \right] + h_b}{R_d + R_0}}$.

The last three equations are dependent and due to their nonlinearity. It would be difficult to solve combined equations (57), (58) and (59) in a general form.

Formally, equation (57) can be used to determine:

$$Q_2 = f_1(Q_1) \tag{60}$$

a substitution into (58) enables Q_3 to be expressed using a new function

$$Q_3 = f_2(Q_1, Q_2) = f_2(Q_1, f_1(Q_1)) = f_2(Q_1), \tag{61}$$

that, after being substituted into (59), would result in an equation for determining Q_1:

$$E_3\left[\left|L_{k3}-f_2\left(Q_1\right)\right|^3-\left|L_{n3}-f_2\left(Q_1\right)\right|^3\right]+E_1\left(L_1-Q_1\right)^2+h_k-h_\text{b}=R_1Q_1^2+R_3\left(f_2\left(Q_1\right)\right)^2. \quad (62)$$

Equation (62) can be solved numerically, e.g. using bisection (dichotomy). Nevertheless, the well-known difficulties of choosing an unambiguous branch of dependencies Q_1 and Q_2 from the difference in negative pressures $h_\text{s}-h_\text{b}$ should not be dismissed. In particular, square values in input equations (56)-(59) should be written as:

$$R_1Q_1^2=R_1Q_1\left|Q_1\right|;\quad R_2Q_2^2=R_2Q_2\left|Q_2\right|; \quad (63)$$

$$E_1\left(L_1-Q_1\right)^2=E_1\left(L_1-Q_1\right)\left|L_1-Q_1\right| \quad 64)$$

etc.

In order to avoid losing necessary real roots, combined equations (57)-(59) will be solved by choosing a negative pressure inside the enclosure of elevator "head" h ($h\equiv h_\text{s}$) and comparing this value with the true negative pressure s:

$$s=R_\text{s}\left(Q_3+Q_2-Q_1\right)\left|Q_3+Q_2-Q_1\right| \quad (65)$$

An iterative approach was used to solve the combined equations in shorter time:

$$h_i=0,5\left(h_{i-1}+s_{i-1}\right), \quad (66)$$

where s_{i-1} is the real negative pressure at determined values of $Q_1=f_1\left(h_{i-1}\right)$, $Q_2=f_2\left(h_{i-1}\right)$ and $Q_3=f_3\left(h_{i-1}\right)$.

Values of Q_1 and Q_2 have been determined using relations:

$$g_1=\frac{R_1}{E_1};\qquad g_2=\frac{R_2}{E_2}; \quad (67)$$

$$t_1=\frac{h_\text{b}-h}{E_1L_1^2};\quad t_2=\frac{h_\text{b}-h}{E_2L_2^2}. \quad (68)$$

At the same time, the unknown flow rates were determined using the formulas:

$$Q_1=\varphi_1v_eS_1=\varphi_1L_1, \quad (69)$$

$$Q_2=\varphi_2v_eS_2=\varphi_2L_2. \quad (70)$$

The values Q_0 and Q_3 were determined by solving equations using the bisection method:

$$f_0=E_0\left[\left|L_{k0}-Q_0\right|^3-\left|L_{n0}-Q_0\right|^3\right]+h_\text{b}-R_0Q_0\left|Q_0\right|=0; \quad (71)$$

$$f_3=E_3\left[\left|L_{k3}-Q_3\right|^3-\left|L_{n3}-Q_3\right|^3\right]+h_\text{c}-h-R_3Q_3\left|Q_3\right|=0. \quad (72)$$

4 CONCLUSIONS

- Analysis of known aerodynamic properties of structurally similar equivalents

(orifices, gates, geometric bodies) makes it possible to conclude that the drag coefficient of a bucket (ζ_b) depends not only on its geometrical shape and the width of the gap between a traveling bucket and elevator enclosure but also on the direction of relative air flow velocity (Fig. 2). When air flows around the back side of a bucket, ζ_b can be determined by analogy with a diaphragm having downstream-chamfered edges. When air flows freely into bucket opening, the drag of the bucket increases several time. However the coefficient ζ_b is dominated by spatial constraints to airflow – the width of the gap between the elevator enclosure walls and buckets. The combined effect of bucket shape, filling degree and flow regimes around them should be determined experimentally.

- Aspiration layouts proposed for elevator handling of grain must make consideration for the predominant effect of ejection forces in ducts. Downward-directed action of ejection head in chutes, together with predominant ejecting properties of the return run with empty buckets, predetermine the use of a classical aspiration layout (Fig. 3): designing for local suction units to evacuate air from the elevator boot cowl and from the cowl at the loading location of the upper (receiving) conveyor or from the internal space of the receiving hopper.
- Fundamental relations for balance equations of air exchange in aspirated cowls (with the purpose of determining necessary aspiration volumes) may be provided by combined equations of air dynamics in four ducts (56)-(59) (or (69)-(72)): inside loading and discharge chutes and in the enclosure of carrying and return runs of the elevator conveyor.

ACKNOWLEDGMENTS

The reported research was funded by Russian Foundation for Basic Research (grant № 16-08-00074 A) and the Grant Council of the President of the Russian Federation (project MD-95.2017.8).

REFERENCES

[1] O.A. Averkova, I.N. Logachev and K.I. Logachev, Ejecting properties of a bucket elevator. *V International Conference on Particle-based Methods. Fundamentals and Applications (PARTICLES 2017)*, pp. 45–56, 2017.

[2] O.A. Averkova, I.N. Logachev and K.I. Logachev, *Cross-flow of air through sealed elevator enclosures. V International Conference on Particle-based Methods. Fundamentals and Applications (PARTICLES 2017)*, pp. 33–44, 2017.

[3] I. N. Logachev and K.I. Logachev. *Industrial Air Quality And Ventilation: Controlling Dust Emissions*. Boca Raton: CRC Press, 2014.

[4] I. N. Logachev, K. I. Logachev and O.A. Averkova. *Local Exhaust Ventilation: Aerodynamic Processes and Calculations of Dust Emissions.* Boca Raton: CRC Press, 2015.

[5] I. E. Idelchik. *Handbook of Hydraulic Resistance*. Begell House Publishers Inc.,U.S., 2007.